Proceedings of the ASME/JSME 2011 8th Thermal Engineering Joint Conference
AJTEC2011
March 13-17, 2011, Honolulu, Hawaii, USA

AJTEC2011-44129

A HYBRID S_N-P_N FORMULATION FOR SOLUTION OF THE BOLTZMANN TRANSPORT EQUATION FOR PHONONS

ARPIT MITTAL
Department of Mechanical Engineering
The Ohio State University, Columbus, OH 43210, USA

SANDIP MAZUMDER*
Department of Mechanical Engineering
The Ohio State University, Columbus, OH 43210, USA

ABSTRACT

A generalized form of the Ballistic-Diffusive Equations (BDE) for approximate solution of the Boltzmann Transport Equation (BTE) for phonons is formulated. The formulation presented here is new and general in the sense that, unlike previously published formulations of the BDE, it does not require *a priori* knowledge of the specific heat capacity of the material. Furthermore, it does not introduce artifacts such as media and ballistic temperatures. As a consequence, the boundary conditions have clear physical meaning. In formulating the BDE, the phonon intensity is split into two components: ballistic and diffusive. The ballistic component is traditionally determined using a viewfactor formulation, while the diffusive component is solved by invoking spherical harmonics expansions. Use of the viewfactor approach for the ballistic component is prohibitive for complex large-scale geometries. Instead, in this work, the ballistic equation is solved using two different established methods that are appropriate for use in complex geometries, namely the discrete ordinates method (DOM), and the control angle discrete ordinates method (CADOM). Results of each method for solving the BDE are compared against benchmark Monte Carlo results, as well as solutions of the BTE using standalone DOM and CADOM for a two-dimensional transient heat conduction problem at various Knudsen numbers. It is found that standalone CADOM (for BTE) and hybrid CADOM-P_1 (for BDE) yield the best accuracy. The hybrid CADOM-P_1 is found to be the best method in terms of computational efficiency.

NOMENCLATURE

f	number distribution function
f_0	equilibrium number distribution function
G	integrated total phonon intensity [Wm^{-2}]
G_b	integrated ballistic component of intensity [Wm^{-2}]
G_d	integrated diffusive component of intensity [Wm^{-2}]
$\hbar$	Dirac constant = 1.0546 x 10^{-34} [$m^2kg.s^{-1}$]
I	total phonon intensity [$Wm^{-2}sr^{-1}$]
I_0	equilibrium phonon intensity [$Wm^{-2}sr^{-1}$]
I_b	ballistic component of phonon intensity [Wm^{-2} sr^{-1}]
I_d	diffusive component of phonon intensity [Wm^{-2} sr^{-1}]
$J_0, \mathbf{J}_1$	constants in spherical harmonics expansion [Eq. (7)]
k_B	Boltzmann constant = 1.381 x 10^{-23} [$m^2kg.s^{-2}K^{-1}$]
Kn	Knudsen number
L	characteristic length scale [m]
$\hat{\mathbf{n}}$	inward pointing unit surface normal vector
p	phonon polarization
$\mathbf{q}$	total heat flux [Wm^{-2}]
$\mathbf{q}_b$	ballistic component of heat flux [Wm^{-2}]
$\mathbf{q}_d$	diffusive component of heat flux [Wm^{-2}]
$\hat{\mathbf{s}}$	unit direction vector
t	time [s]
t^*	non-dimensional time
T	thermodynamic temperature [K]

Greek

$\mathbf{v}_g$	phonon group velocity vector [m/s]
τ	overall scattering time scale [s]
ω	angular frequency [rad/s]
Ω	solid angle (sr)
σ_p	Stefan-Boltzmann constant for phonons [$Wm^{-2}K^{-4}$]

INTRODUCTION

The efficient removal of heat from modern-day solid-state electronic and optoelectronic devices is a daunting task, and overheating is one of the most common causes of device failure. Modeling thermal transport in micro- and nano- scale crystalline materials can provide fundamental understanding of the mechanisms of heat conduction in semiconductor devices.

The mean free path of the energy-carrying acoustic wave packets (or phonons) in silicon at room temperature is approximately 300 nm [1]. On the other hand, characteristic

*E-mail: mazumder.2@osu.edu, Member ASME

dimensions of modern semiconductor devices range from a few tens of nanometers to a few hundreds of nanometers [2]. Consequently, heat conduction in such devices cannot be described adequately using continuum equations, namely the Fourier law of heat conduction. Non-equilibrium heat conduction has been successfully modeled in the past using the semi-classical Boltzmann Transport Equation (BTE) for phonons.

Even if the physics of phonons were to be neglected, *i.e.*, no dispersion, no polarization, frequency-independent (or gray), the BTE is a six-dimensional partial differential equation: 3 spatial coordinates, 2 angular coordinates, and time. This high dimensionality of the BTE makes it very challenging to solve, even for simple one-dimensional (1D) films. Traditionally, stochastic methods, such as the Monte Carlo method, have found success in solving high-dimensional partial differential equations. For example, the Monte Carlo method has been successfully used to solve the BTE or its variants for rarefied gas (also known as direct simulation Monte Carlo or DSMC) [3], photons (or radiative transport) [4,5], electrons, and other charge carriers [6,7]. The advantage of the Monte Carlo method is that it is tractable and almost linearly scalable for large number of dimensions, and is amenable to addressing complex physics *via* interactions between the stochastic samples. The shortcoming of this method is that it is prohibitively expensive for practical engineering applications. In the case of phonon transport, for example, studies [8-10] have shown that even simulation of heat conduction in a 1D thin film can require several tens of hours of CPU time. Perhaps, the most notable disadvantage of using the Monte Carlo method is that the solution inherently contains statistical errors. While these errors can be reduced by using a large number of stochastic samples, they cannot be completely eliminated. Often, the errors are large enough to cause spurious oscillations and non-convergence, if the Monte Carlo solver were to be coupled to a deterministic solver for some other aspect of the problem, such as for charge carrier transport. In light of these issues, it is fair to contend that the Monte Carlo method is useful for generating benchmark solutions for simple problems but not practical for simulating non-equilibrium heat conduction in large-scale devices, and deterministic methods for solving the BTE are desired.

Deterministic solution of the BTE for phonons in multi-dimensional geometry has been attempted and brought to the limelight primarily by Murthy and co-workers [11-13]. The algorithms used by Murthy and co-workers are directly adapted from existing algorithms in neutron and photon (radiation) transport. Most notably, this particular group has used the Discrete Ordinates Method (DOM) [14] based on the S_N approximation, and its variants. Over the years, the algorithms have been refined to improve accuracy and efficiency. For example, a switch has been made from the standard DOM to the so-called Control Angle Discrete Ordinates Method (CADOM) [15,16] to eliminate so-called "ray effects" and "false scattering" [17]. Also, higher-order and more robust discretization schemes in space, such as the SMART scheme [18], has been introduced [11,12] to improve accuracy and convergence. While the discrete ordinates method has shown tremendous promise for solution of the BTE for phonons, it is still quite expensive. In particular, in the ballistic regime (high Knudsen number), a large number of directions (or control angles) have to be used to attain acceptable accuracy, as has been shown in previously published results [11-13], and will also be shown in this article. This implies solution of a large number of partial differential equations. In the diffusive regime (low Knudsen number), on the other hand, since phonon transport is diffusive, use of DOM with high angular resolution is wasteful and, perhaps, use of a simpler diffusive approximation is warranted for improved efficiency. One method which has often been used to solve the BTE is the method of spherical harmonics (or P_N approximation). In this method, the angular directions are not discretized. Rather, spherical harmonic basis functions, namely Legendre polynomials, are used to capture the angular variations in the intensity analytically. The lowest order spherical harmonics approximation, namely the P_1 approximation, reduces the BTE to a single Helmholtz equation with Robin boundary conditions, making it an attractive choice for solution of the BTE since only one partial differential equation has to be solved, as opposed to several tens in the discrete ordinates method. Unfortunately, the P_1 approximation is reasonably accurate only in the diffusive (low Knudsen number) regime, and its accuracy at intermediate or high Knudsen numbers is unacceptable, as conclusively demonstrated for photon (radiation) transport [19,20]. Therefore, the P_1 approximation is inappropriate for solution of the BTE in truly non-equilibrium scenarios. Higher order P_N approximations, as recently formulated for radiation transport [21], may be used. However, use of higher order P_N approximations is significantly more cumbersome than using the P_1 approximation [20,21], and the benefits in terms of improved accuracy is often marginal [20].

The Modified Differential Approximation (MDA) was proposed to remove the shortcomings of the P_1 approximation for intermediate and high Knudsen numbers. In this method, first proposed by Olfe [22] and later generalized for radiation transport by Modest [23], the intensity of the energy carrier is split into two components: ballistic and diffusive. The ballistic component is determined using a surface-to-surface exchange formulation that employs geometric viewfactors, while the spherical harmonics approximation is invoked for the diffusive component, for which it is justifiably applicable. The result is a hybrid approach that is expected to be efficient and accurate at all Knudsen numbers. In the past decade, the MDA approach has been adopted for solution of the BTE for phonons by Chen and co-workers [24-26], resulting in the so-called ballistic-diffusive equations (BDE) of phonon transport. In the BDE formulation proposed by Chen and co-workers [24-26], the specific heat capacity of the material appears as an input. This makes direct comparison with results of the BTE difficult, since the specific heat capacity of the material is not an input in the BTE. Secondly, Chen and co-workers introduce artificial temperatures, namely ballistic and media temperatures, in their formulation. These temperatures do not have a physical meaning and are introduced as mathematical artifacts. As a result, they make the formulation—in particular, the boundary conditions—difficult to understand and interpret. A final point

to note is that the surface-to-surface exchange formulation using geometric viewfactors is prohibitive on two counts: (1) it is very expensive and tedious for complex multi-dimensional geometries in which case determination of the viewfactors itself is a monumental task [27], and (2) all surfaces in a heat conduction simulations are not necessarily diffuse, and therefore, the use of diffuse geometric viewfactors is limiting in its scope.

In this paper, we present a new hybrid formulation (or BDE formulation) for solution of the BTE. The new formulation does not require *a priori* knowledge of the specific heat capacity of the material, and requires the exact same inputs as the original BTE, making direct comparison with the BTE possible. While the new formulation is based upon the same intensity splitting philosophy originally proposed by Olfe [22] for development of the MDA formulation, the resulting BDEs are solved using procedures that are general enough to be applicable to any arbitrary geometry with arbitrary thermal boundary conditions. The ballistic component is determined, in this case, using the Discrete Ordinates Method (DOM) and its variants such as the Control Angle Discrete Ordinates Method (CADOM), while the diffusive component is determined by invoking the P_N approximation. The result is a hybrid S_N-P_N formulation that is flexible enough to allow any accuracy order. As part of this study, direct comparisons are made with benchmark results obtained by solving the BTE using the Monte Carlo method, as well as standalone DOM or CADOM for a transient heat conduction problems at various Knudsen numbers. While the results shown here are for the gray BTE, the formulation is applicable to the non-gray (frequency dependent) BTE without additional modifications.

THEORY AND SOLUTION PROCEDURE

Quantized lattice vibrations or phonons are the predominant carriers of thermal energy in semiconductor materials [28]. If the mean free path of the traveling phonons is larger than the characteristic dimension of the device being modeled, thermodynamic equilibrium ceases to exist, and thus, the Fourier law of heat conduction is invalid.

The Boltzmann Transport Equation (BTE) is a semi-classical equation, and has been successfully used to model particles that interact with each other *via* short range forces and follow a statistical distribution [2,28]. Phonons follow Bose-Einstein statistics and interact with each other *via* scattering processes, and therefore, can be modeled using the BTE, which may be written as [2]

$$\frac{\partial f}{\partial t} + \mathbf{v}_g \bullet \nabla f = \left[\frac{\partial f}{\partial t}\right]_{scattering} \tag{1}$$

where f is the distribution function of an ensemble of phonons, and $\mathbf{v}_g$ is the group velocity. The left side of Eq. (1) represents change of the distribution function due to motion (or drift), whereas the right hand side represents change in the distribution function due to collisions (or scattering). Drift causes the phonon energy distribution function to deviate from equilibrium, while collisions tend to restore equilibrium.

Prior to solution of the BTE for phonons, it is necessary to formulate the right-hand-side of Eq. (1). This scattering term is complicated if all possible scattering mechanisms are considered rigorously. Due to the complexity of the scattering term, simplifications and approximations have to be made to the BTE before it can be solved. The most common approximation used to simplify the BTE is the single relaxation time approximation, whereby the scattering term is expressed as

$$\left[\frac{\partial f}{\partial t}\right]_{scattering} = \frac{f - f_0}{\tau} \tag{2}$$

where f_0 is the equilibrium distribution function (*i.e.*, the Bose-Einstein distribution function), and τ is the overall scattering time-scale of the phonon due to all scattering processes in combination. For an isotropic wave vector space, the distribution function, f, is a function of seven independent variables, *i.e.*, $f = f(t, \mathbf{r}, \hat{\mathbf{s}}, \omega)$, where t is time, and ω is the angular frequency. The space vector $\mathbf{r}$ has 3 components, while the direction vector $\hat{\mathbf{s}}$ has 2 components, namely the polar angle θ, and the azimuthal angle ψ. The equilibrium Bose-Einstein distribution, f_0, on the other hand, is independent of direction, *i.e.*, $f_0 = f_0(t, \mathbf{r}, \omega)$. The group velocity, $\mathbf{v}_g$, is a function of direction, angular frequency and temperature, *i.e.*, $\mathbf{v}_g = \mathbf{v}_g(\hat{\mathbf{s}}, \omega, T)$, while the scattering time-scale, τ, is a function of angular frequency and temperature, *i.e.*, $\tau = \tau(\omega, T)$. Equations (1) and (2) can be combined and written in terms of the phonon intensity as follows [25]:

$$\frac{\partial I}{\partial t} + \mathbf{v}_g \bullet \nabla I = \frac{\partial I}{\partial t} + \left|\mathbf{v}_g\right| \nabla \bullet (I\hat{\mathbf{s}}) = \frac{I_0 - I}{\tau} \tag{3}$$

where $\mathbf{v}_g = \left|\mathbf{v}_g\right| \hat{\mathbf{s}}$, and the phonon intensity is defined as

$$I = I(t, \mathbf{r}, \hat{\mathbf{s}}, \omega) = \left|\mathbf{v}_g\right| \hbar\omega f \; D(\omega) / 4\pi \tag{4}$$

where $D(\omega)$ is the phonon density of states per unit volume and $\hbar$ is the Dirac constant.

Derivation of Ballistic-Diffusive Equation (BDE)

Following, the intensity splitting philosophy of Olfe [22], the phonon intensity is next split into two components:

$$I(t, \mathbf{r}, \hat{\mathbf{s}}, \omega) = I_b(t, \mathbf{r}, \hat{\mathbf{s}}, \omega) + I_d(t, \mathbf{r}, \hat{\mathbf{s}}, \omega) \tag{5}$$

where I_b and I_d are ballistic and diffusive components, respectively. The ballistic component represents phonons emitted from the boundaries and scattered, while the diffuse component represents phonons that are emitted from within the medium and scattered. The former component is highly directional in nature since phonons follow a direct line of sight from a hot surface to a cold surface, while the latter component is directionally weak since emission is inherently isotropic. Substitution of Eq. (5) into Eq. (3), followed by separation of the ballistic and diffusive components, yields:

$$\text{Ballistic: } \frac{\partial I_b}{\partial t} + \left|\mathbf{v}_g\right| \nabla \bullet (I_b \hat{\mathbf{s}}) = -\frac{I_b}{\tau} \tag{6a}$$

Diffusive: $\frac{\partial I_d}{\partial t} + \left|\mathbf{v}_g\right| \nabla\bullet(I_d\,\hat{\mathbf{s}}) = \frac{I_0 - I_d}{\tau}$ (6b)

Since the diffusive intensity field is a directionally weak function, it is justifiable to invoke the first order P_N approximation for directional variation in the intensity. Thus, using the P_1 approximation, the diffusive intensity field may be written as [19,25]

$$I_d(t,\mathbf{r},\hat{\mathbf{s}},\omega) = J_0(t,\mathbf{r},\omega) + \mathbf{J}_1(t,\mathbf{r},\omega)\bullet\hat{\mathbf{s}} \quad (7)$$

where J_0 is a direction independent scalar coefficient, and $\mathbf{J}_1$ is a direction independent vector coefficient. The dot product with the direction vector renders the second term in Eq. (7) a scalar. Substitution of Eq. (6b) into Eq. (7) yields

$$\frac{\partial[J_0 + \mathbf{J}_1\bullet\hat{\mathbf{s}}]}{\partial t} + \left|\mathbf{v}_g\right| \nabla\bullet([J_0 + \mathbf{J}_1\bullet\hat{\mathbf{s}}]\,\hat{\mathbf{s}}) = \frac{I_0 - [J_0 + \mathbf{J}_1\bullet\hat{\mathbf{s}}]}{\tau} \quad (8)$$

Integrating Eq. (8) over the entire solid angle 4π, and noting that $\int_{4\pi}\hat{\mathbf{s}}\,d\Omega = 0$ and $\int_{4\pi}\hat{\mathbf{s}}\hat{\mathbf{s}}\,d\Omega = \frac{4\pi}{3}\delta$ (δ is the identity tensor) [19], we get

$$\frac{\partial J_0}{\partial t} + \left|\mathbf{v}_g\right| \nabla\bullet(\frac{1}{3}\mathbf{J}_1) = \frac{I_0 - J_0}{\tau} \quad (9)$$

Equation (9) has two unknowns, namely J_0 and $\mathbf{J}_1$, and cannot be solved. In order to derive another additional equation to close the system of equations, we multiply Eq. (8) by $\hat{\mathbf{s}}$ and then integrate the resulting equation over the entire solid angle 4π. After tedious algebra, this yields

$$\frac{\partial \mathbf{J}_1}{\partial t} + \left|\mathbf{v}_g\right| \nabla J_0 = -\frac{\mathbf{J}_1}{\tau} \quad (10)$$

Equations (9) and (10) represent two equations with 2 unknowns, namely J_0 and $\mathbf{J}_1$. In principle, this equation system is closed, and can be solved to determine the two unknowns. Unfortunately, since Eq. (10) is a vector equation, it is quite tedious to solve. In order to eliminate $\mathbf{J}_1$ in favor of J_0 we first differentiate Eq. (9) with respect to time, yielding

$$\frac{\partial^2 J_0}{\partial t^2} + \frac{\left|\mathbf{v}_g\right|}{3}\frac{\partial}{\partial t}[\nabla\bullet\mathbf{J}_1] = \frac{1}{\tau}\left[\frac{\partial I_0}{\partial t} - \frac{\partial J_0}{\partial t}\right] \quad (11)$$

Next, we take divergence of Eq. (10), resulting in

$$\frac{\partial}{\partial t}[\nabla\bullet\mathbf{J}_1] + \left|\mathbf{v}_g\right| \nabla^2 J_0 = -\frac{\nabla\bullet\mathbf{J}_1}{\tau} \quad (12)$$

Substitution of Eq. (12) into Eq. (11) yields

$$\frac{\partial^2 J_0}{\partial t^2} + \frac{1}{\tau}\frac{\partial J_0}{\partial t} - \frac{\left|\mathbf{v}_g\right|}{3\tau} \nabla\bullet\mathbf{J}_1 - \frac{\left|\mathbf{v}_g\right|^2}{3}\nabla^2 J_0 = \frac{1}{\tau}\frac{\partial I_0}{\partial t} \quad (13)$$

Substitution of Eq. (9) into Eq. (13) yields

$$\frac{\partial^2 J_0}{\partial t^2} + \frac{2}{\tau}\frac{\partial J_0}{\partial t} + \frac{1}{\tau^2}\ J_0 - \frac{\left|\mathbf{v}_g\right|^2}{3}\nabla^2 J_0 = \frac{1}{\tau^2}\ I_0 + \frac{1}{\tau}\frac{\partial I_0}{\partial t} \quad (14)$$

Equation (14) can be solved to determine J_0. In principle, once J_0 has been determined, Eq. (10) can be solved to determine $\mathbf{J}_1$, and finally, Eq. (7) provides the diffuse component of the phonon intensity field. However, for heat transfer calculations, we are rarely interested in the intensity. More often, we are interested in determining the heat flux, the integrated (over all solid angles) intensity, and the divergence of the heat flux. Using the P_1 approximation, the integrated diffusive intensity field may be written as

$$G_d = \int_{4\pi} I_d\,d\Omega = \int_{4\pi}[J_0 + \mathbf{J}_1\bullet\hat{\mathbf{s}}]d\Omega = 4\pi J_0 \quad (15)$$

since $\mathbf{J}_1$ is independent of direction, and $\int_{4\pi}\hat{\mathbf{s}}\,d\Omega = 0$. Substitution of Eq. (15) into Eq. (14) yields an equation for the directionally integrated diffusive component of the phonon intensity, G_d:

$$\frac{\partial^2 G_d}{\partial t^2} + \frac{2}{\tau}\frac{\partial G_d}{\partial t} + \frac{1}{\tau^2}\ G_d - \frac{\left|\mathbf{v}_g\right|^2}{3}\nabla^2 G_d = \frac{4\pi}{\tau^2}\ I_0 + \frac{4\pi}{\tau}\frac{\partial I_0}{\partial t} \quad (16)$$

Equation (16) is the governing equation for the diffusive component of the phonon intensity. It is preferable over Eq. (14) since the quantity G_d has a physical meaning (as discussed above), while J_0 is simply a mathematical quantity without any physical meaning. We conclude this discussion on derivation of the BDE by noting that the ballistic component of the intensity can be determined by solving Eq. (6a), while the diffusive component can be determined by solving Eq. (16), albeit in integrated form. As to why solution of the integrated intensity (as opposed to the directional intensity) is sufficient for heat transfer calculations will become clear in the next section. One final point to note is that solution of both Eq. (6a) and Eq. (16) requires boundary conditions, and the boundary conditions are discussed in a later section.

Heat Flux, Divergence of Heat Flux, and Temperature

The ultimate goal of any heat transfer calculation is to predict the normal heat flux at the boundaries and the temperature distribution inside the medium. The relationship between these engineering quantities and the phonon intensity is discussed in this section.

The heat flux is related to the phonon intensity by the relationship [19]

$$\mathbf{q} = \int_{4\pi} I\hat{\mathbf{s}}\,d\Omega \quad (17)$$

which, upon application of the intensity splitting philosophy [Eq. (5)], becomes

$$\mathbf{q} = \int_{4\pi}(I_b + I_d)\hat{\mathbf{s}}\,d\Omega = \int_{4\pi} I_b\hat{\mathbf{s}}\,d\Omega + \int_{4\pi} I_d\hat{\mathbf{s}}\,d\Omega = \mathbf{q}_b + \mathbf{q}_d \quad (18)$$

While the solution of the BTE or the BDE provides a mechanism to determine the heat flux, in order to determine the temperature distribution, one must apply the first law of thermodynamics. For static media, the first law may be written as [29]

$$\frac{\partial U}{\partial t} = -\nabla\bullet\mathbf{q} + \dot{q}_{gen} = -\nabla\bullet\mathbf{q}_b - \nabla\bullet\mathbf{q}_d + \dot{q}_{gen} \quad (19)$$

where U is the internal energy per unit volume and $\dot{q}_{gen}$ is the heat generation rate per unit volume due to other mechanisms, such as electron-phonon or photon-phonon interactions *etc*. Equation (18) has been made use of to derive the last part of

Eq. (19). Invoking the P_1 approximation to the diffusive component of the heat flux in Eq. (18), we obtain

$$\mathbf{q}_d = \int_{4\pi} I_d \hat{\mathbf{s}}\, d\Omega = \int_{4\pi} (J_0 + \mathbf{J}_1 \bullet \hat{\mathbf{s}})\hat{\mathbf{s}}\, d\Omega = \frac{4\pi}{3}\mathbf{J}_1 \tag{20}$$

Taking divergence of Eq. (20) yields

$$\nabla \bullet \mathbf{q}_d = \frac{4\pi}{3}\nabla \bullet \mathbf{J}_1 \tag{21}$$

Substitution of Eq. (9) and Eq. (15) into Eq. (21) yields

$$\nabla \bullet \mathbf{q}_d = \frac{4\pi}{|\boldsymbol{\upsilon}_g|}\left[\frac{I_0}{\tau} - \frac{J_0}{\tau} - \frac{\partial J_0}{\partial t}\right] = \frac{1}{|\boldsymbol{\upsilon}_g|}\left[\frac{4\pi I_0}{\tau} - \frac{G_d}{\tau} - \frac{\partial G_d}{\partial t}\right] \tag{22}$$

In order to derive an expression for the divergence of the ballistic component of the heat flux, we integrate Eq. (6a) over the all solid angles, yielding

$$\frac{\partial}{\partial t}\left[\int_{4\pi} I_b\, d\Omega\right] + |\boldsymbol{\upsilon}_g|\ \nabla \bullet \left(\int_{4\pi} I_b \hat{\mathbf{s}}\, d\Omega\right) = -\frac{1}{\tau}\left[\int_{4\pi} I_b\, d\Omega\right] \tag{23}$$

Defining an integrated ballistic intensity as $G_b = \int_{4\pi} I_b\, d\Omega$ and using Eq. (18), we get

$$\frac{\partial G_b}{\partial t} + |\boldsymbol{\upsilon}_g|\ \nabla \bullet \mathbf{q}_b = -\frac{G_b}{\tau} \tag{24}$$

Substitution of Eqs. (22) and (24) into Eq. (19) yields

$$\begin{aligned}\frac{\partial U}{\partial t} &= \frac{1}{|\boldsymbol{\upsilon}_g|}\left[\frac{G_b}{\tau} + \frac{\partial G_b}{\partial t}\right] - \frac{1}{|\boldsymbol{\upsilon}_g|}\left[\frac{4\pi I_0}{\tau} - \frac{G_d}{\tau} - \frac{\partial G_b}{\partial t}\right] + \dot{q}_{gen} \\ &= -\frac{1}{|\boldsymbol{\upsilon}_g|}\left[\frac{4\pi I_0}{\tau} - \frac{G}{\tau} - \frac{\partial G}{\partial t}\right] + \dot{q}_{gen}\end{aligned} \tag{25}$$

where $G = G_b + G_d$ is the total integrated (over all solid angles) phonon intensity.

The internal energy of a crystalline material is related to its temperature through the Bose-Einstein distribution and its density of state [2]

$$U = \sum_p \int_{\omega_{\min}}^{\omega_{\max}} \frac{\hbar\omega D(\omega, p)}{\exp[\hbar\omega / k_B T] - 1} d\omega \tag{26}$$

where the summation is over all polarization branches, and k_B is the Boltzmann constant. If Eq. (26) is substituted into Eq. (25), it becomes clear that determination of the temperature field will require solution of a non-linear equation. Under the assumption of a linear dispersion relationship and a single polarization branch, we obtain the following relationships

$$U = \frac{4\sigma_p T^4}{|\boldsymbol{\upsilon}_g|}; \quad I_0 = \frac{\sigma_p T^4}{\pi} \tag{27}$$

where $\sigma_p = \pi^2 k_B^4 / 40\hbar^3 |\boldsymbol{\upsilon}_g|^2$ is the so-called Stefan-Boltzmann constant for phonons [2]. It is worth noting that the expression for the Stefan-Boltzmann constant includes the group velocity. Only under the assumption of a linear dispersion relationship (or no dispersion) is the group velocity a constant. Consequently, the Stefan-Boltzmann constant for phonons, unlike its photon counterpart, is not a true constant, but one that is applicable only under the assumption of no dispersion.

Boundary Conditions for the BDE

As discussed in Section 2.1, determination of the phonon intensity requires solution to Eqs. (6a) and (16). Equation (6a) is a first-order partial differential equation in space, and therefore, requires only one boundary condition. Physically, the intensity is forward propagating, and is required only at the point of emission on the boundary. For sub-micron heat conduction simulations, two kinds of boundary conditions are relevant. The first kind is where the boundary is a thermalizing boundary, *i.e.*, one that is analogous to a black surface for thermal radiation. It emits phonons based on the equilibrium energy distribution and absorbs any phonons that strike it. Mathematically, this implies

$$I_b(t, \mathbf{r} = \mathbf{r}_w, \hat{\mathbf{s}}, \omega) = I_0(t, \mathbf{r} = \mathbf{r}_w, \omega) \tag{28}$$

where $\mathbf{r}_w$ is the location of the boundary (or wall). The second kind is an adiabatic boundary that reflects all phonons striking it, and absorbs none. The reflection may be diffuse, specular, or partially specular. Depending on the reflection characteristics of the surface, the total incident radiation to the boundary is re-distributed into specific directions. The procedure on how to apply reflection boundary conditions in the context of the DOM or the CADOM, which are the methods employed here, is available elsewhere [11,12], and is omitted here for the sake of brevity.

The boundary conditions for the diffusive component of the phonon intensity are not as straightforward. Since we are solving the governing equation for the integrated intensity, G_d, rather than the intensity itself, the boundary conditions need to be formulated accordingly. The most common procedure to develop boundary conditions for G_d is to apply Marshak's procedure [19]. Essentially, this amounts to satisfying flux conservation at the boundaries. The heat flux normal to a boundary is the net effect of phonons emitted from the boundary and the phonons absorbed by the boundary. Thus

$$\begin{aligned}\mathbf{q} \bullet \hat{\mathbf{n}} = \mathbf{q}_b \bullet \hat{\mathbf{n}} + \mathbf{q}_d \bullet \hat{\mathbf{n}} &= \underbrace{\int_{\hat{\mathbf{n}}\bullet\hat{\mathbf{s}}>0} I_0\, \hat{\mathbf{n}}\bullet\hat{\mathbf{s}}\, d\Omega}_{\text{outgoing}} - \underbrace{\int_{\hat{\mathbf{n}}\bullet\hat{\mathbf{s}}<0} I\, \hat{\mathbf{n}}\bullet\hat{\mathbf{s}}\, d\Omega}_{\text{incoming}} \\ &= \pi I_0 - \int_{\hat{\mathbf{n}}\bullet\hat{\mathbf{s}}<0} I_b\, \hat{\mathbf{n}}\bullet\hat{\mathbf{s}}\, d\Omega - \int_{\hat{\mathbf{n}}\bullet\hat{\mathbf{s}}<0} I_d\, \hat{\mathbf{n}}\bullet\hat{\mathbf{s}}\, d\Omega\end{aligned} \tag{29}$$

where $\hat{\mathbf{n}}$ is the inward facing surface normal to the boundary. If the ballistic component of the heat flux at the boundaries is written as

$$\mathbf{q}_b \bullet \hat{\mathbf{n}} = \pi I_0 - \int_{\hat{\mathbf{n}}\bullet\hat{\mathbf{s}}<0} I_b\, \hat{\mathbf{n}}\bullet\hat{\mathbf{s}}\, d\Omega \tag{30}$$

it follows from Eqs. (29) and (30) that the diffuse component is

$$\mathbf{q}_d \bullet \hat{\mathbf{n}} = -\int_{\hat{\mathbf{n}}\bullet\hat{\mathbf{s}}<0} I_d\, \hat{\mathbf{n}}\bullet\hat{\mathbf{s}}\, d\Omega \tag{31}$$

Equation (30) is consistent with the intensity boundary conditions discussed above for the ballistic component. Application of the P_1 approximation [Eq. (7)] to Eq. (31), followed by substitution of Eq. (20) yields

$$\begin{aligned}\mathbf{q}_d \bullet \hat{\mathbf{n}} &= -\int_{\hat{\mathbf{n}}\bullet\hat{\mathbf{s}}<0} [J_0 + \mathbf{J}_1 \bullet \hat{\mathbf{s}}]\hat{\mathbf{n}}\bullet\hat{\mathbf{s}}\, d\Omega \\ &= -(\pi J_0 - \frac{2\pi}{3}\mathbf{J}_1 \bullet \hat{\mathbf{n}}) = -(\pi J_0 - \frac{1}{2}\mathbf{q}_d \bullet \hat{\mathbf{n}})\end{aligned} \tag{32}$$

Upon rearrangement of Eq. (32), we obtain

$$\mathbf{q}_d \bullet \hat{\mathbf{n}} = -2\pi J_0 \tag{33}$$

Substituting Eq. (20) in Eq. (10), we obtain

$$\frac{\partial \mathbf{q}_d}{\partial t} + \left|\mathbf{v}_g\right| \nabla\left(\frac{4\pi}{3} J_0\right) = -\frac{\mathbf{q}_d}{\tau} \tag{34}$$

Performing a dot product of $\hat{\mathbf{n}}$ with Eq. (34), followed by substitution of Eq. (33) and Eq. (15) into the resulting equation yields

$$\frac{\partial G_d}{\partial t} - \frac{2}{3}\left|\mathbf{v}_g\right| \hat{\mathbf{n}} \bullet \nabla G_d = -\frac{G_d}{\tau} \tag{35}$$

Equation (35) represents the boundary condition for Eq. (16). It is a boundary condition of the third kind (Robin type) and is applicable to all non-adiabatic boundaries of the computational domain. For adiabatic boundaries or symmetry plains, the diffuse component of the heat flux must be set to zero, and it follows from Eqs. (33) and (15) that $G_d = 0$ at adiabatic boundaries.

Solution Algorithm and Numerical Procedure

The preceding sections outline the governing equations that need to be solved and the associated boundary conditions for the BDE. In order to attain the solution to a heat transfer problem using this formulation, the equations need to be solved in a certain sequence, which is described below:

Step 1: Set initial conditions for temperature (internal energy), and the two components of the phonon intensity, namely I_b and G_d

Step 2: Solve for the ballistic component of the phonon intensity, I_b, using Eq. (6a) subject the boundary condition provided in Eq. (28)

Step 3: Compute the integrated ballistic component of the phonon intensity using $G_b = \int_{4\pi} I_b \, d\Omega$

Step 4: Guess the temperature distribution within the whole computational domain. This provides an initial estimate for the equilibrium energy distribution, I_0, through Eq. (27).

Step 5: Determine the integrated diffusive component of the phonon intensity, G_d, by solving Eq. (16) subject to the boundary condition given by Eq. (35).

Step 6: Solve the overall energy balance equation [Eq. (25)]. In conjunction with Eq. (26) or Eq. (27), this provides the new temperature distribution.

Step 7: Repeat steps 5 and 6 until convergence (*i.e.*, temperature stops changing within that particular time-step).

Step 8: Compute heat fluxes at boundaries using Eqs. (30), (33) and (15)

Step 9: Proceed to next time-step and repeat Steps 2-8.

The two most critical and time-consuming steps in the algorithm just described are the determination of the ballistic component of the phonon intensity (Step 2) and the diffusive component of the phonon intensity (Step 5). As mentioned earlier, the ballistic component is traditionally determined by using a surface-to-surface exchange formulation that makes use of geometric viewfactors between diffuse surfaces, as was done by Chen and co-workers [24-26]. This approach is restrictive because it is difficult to mix diffuse and specular surfaces, as is always prevalent in practical problems. Secondly, such a method is prohibitively expensive when the geometry is complex (with obstructions and 3D), as has been demonstrated recently for photon transport [27]. In light of these shortcomings of the traditional viewfactor based approach, we chose to use the Discrete Ordinates Method (DOM) and the Control Angle Discrete Ordinates Method (CADOM) for the solution of Eq. (6a). CADOM is preferable over DOM for ballistic (high Knudsen number) cases because it alleviates ray effects. The numerical procedures for discretization of the Boltzmann Transport Equation for phonons using either DOM or CADOM on an unstructured mesh are reported elsewhere [11,30], and are omitted here for the sake of brevity. In this work, both Eqs. (6a) and (16) are discretized on an unstructured mesh of arbitrary topology using the finite-volume procedure. The resulting algebraic equations are solved using the Generalized Minimum Residual (GMRES) solver [31] after incomplete LU (ILU) pre-conditioning.

An important attribute of the numerical algorithm described above is that only Steps 5 and 6 have to be repeated. The ballistic equation (directional discrete ordinates equations) is solved only once, *i.e.*, Step 2 is executed only once. Change of the medium's temperature requires repeated solution of only the diffuse component of the phonon intensity (Step 5). This implies that in this hybrid method, only a single partial differential equation [Eq. (16)] has to be solved repeatedly within the outer iteration loop that updates temperature of the medium. In contrast, if the DOM or CADOM is used directly for the solution of the BTE, all directional equations in the DOM or CADOM method have to be solved repeatedly. Clearly, this is a notable advantage of the hybrid method (or BDE) over direct solution of the BTE, in terms of computational efficiency. Another advantage of the hybrid approach is that the governing equation for the ballistic component, namely Eq. (6a), is source-less, as indicated by the lack of the I_0-containing term. This makes it more amenable to numerical solution in comparison to the original BTE [Eq. (3)], which has this source present.

Non-Dimensional Form of BDE and Knudsen Number

The degree of non-equilibrium in any non-equilibrium coupled transport-scattering/collision process is dictated by the Knudsen number. In the context of heat conduction, the Knudsen number is defined as the ratio of the mean free path of the energy carrying phonons to the characteristic dimension. If L is the characteristic length scale of the device being modeled, and Λ is the mean free path, then the Knudsen number is defined as

$$Kn = \frac{\Lambda}{L} = \frac{\left|\mathbf{v}_g\right|\tau}{L} \tag{36}$$

Under the gray (frequency independent) assumption, both the scattering time scale, τ, as well as the group velocity, $\left|\mathbf{v}_g\right|$, are constants. Consequently, the Knudsen number is a constant under the gray assumption.

Introducing the non-dimensional time and space variables, namely $x^* = x/L; t^* = t/\tau$, it is easy to show that Eqs. (6a) and (16) can be re-written in the following form

$$\frac{\partial I_b}{\partial t^*} + Kn\nabla^* \bullet (I_b \hat{\mathbf{s}}) = -I_b \tag{37a}$$

$$\frac{\partial^2 G_d}{\partial t^{*2}} + 2\frac{\partial G_d}{\partial t^*} + G_d - \frac{Kn^2}{3}\nabla^{*2} G_d = 4\pi I_0 + 4\pi \frac{\partial I_0}{\partial t^*} \tag{37b}$$

Equation (37) clearly shows that the Knudsen number is the only parameter that dictates the solution of the governing equations.

In summary, a new set of ballistic-diffusive equations have been developed starting from the Boltzmann Transport Equation for phonons. The solution to these equations does not require any inputs other than the boundary conditions, initial conditions, and the Knudsen number. In the following section, a test case is presented to verify and validate the new formulation by comparing its results with the solutions of the original Boltzmann Transport Equation.

RESULTS AND DISCUSSION

In order to test the new hybrid formulation, a two-dimensional transient heat conduction problem was considered. The geometry and boundary conditions are shown in Fig.1. This particular problem is similar to the one considered by Yang *et al.* [26]. The heater is set to a temperature T_H = 200K, while the walls are set to a temperature of T_C = 100K. The overall size of the cavity and the phonon group velocity were fixed, and the scattering time scale was adjusted to vary the Knudsen number. For validation of the results, the BTE was solved using the Monte Carlo method, in addition to the various deterministic methods. For the Monte Carlo simulations, 4 million stochastic samples (phonon bundles) were used. Each solution was time-marched until steady state was attained. A non-dimensional time step equal to 10^{-4} was used. Within each time-step, six orders of magnitude convergence was enforced. For most cases, this required between 5 and 10 iterations. For DOM, the S_8 approximation (40 angles in 2D) was used, and an equivalent number of control angles were used for CADOM.

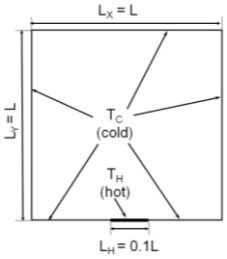

Figure 1: Geometry and boundary conditions

Figure 2(a) shows the time evolution of the temperature profiles along the centerline of the cavity (from bottom to top) for a Knudsen number of 0.01. The corresponding heat fluxes at steady state along the bottom wall are shown in Fig. 2(b). It is clear from this figure that all methods are fairly accurate for this acoustically thick (diffusive limit) case. The solution of the BTE by DOM or CADOM matches exactly with Monte Carlo results, while the solution of the BDE using the hybrid formulation produces slight errors. Minor differences are also observed in the flux predictions between the two cases. In Fig. 2(b), results of the hybrid viewfactor based BDE, as used traditionally, are also shown, and they appear to be quite accurate, as well.

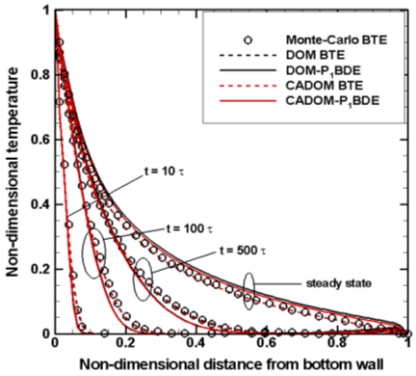

(a) Temperature along centerline

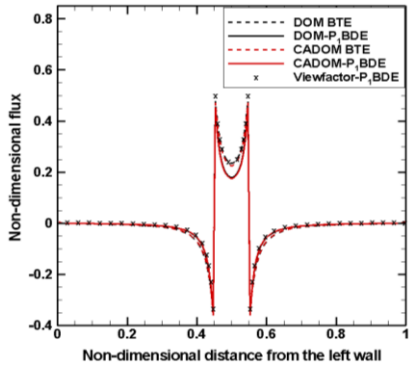

(b) Heat flux along bottom wall

Figure 2: Non-dimensional temperature [= $(T-T_C)/(T_H-T_C)$] and heat flux [= $q/\sigma_p(T_H^4-T_C^4)$] for Knudsen number of 0.01 (diffusive limit)

Centerline temperature distributions for Knudsen number equal to unity (intermediate acoustic thickness) are shown in Fig. 3. In this case, the results obtained using the standard discrete ordinates method, either for BTE or BDE, are not very accurate. This is due to the "ray effect," as will be discussed in detail shortly. The hybrid method based on CADOM (CADOM-P_1) matches solutions of the BTE almost exactly. A slight slip is observed near the walls—an indication of the onset of non-equilibrium transport.

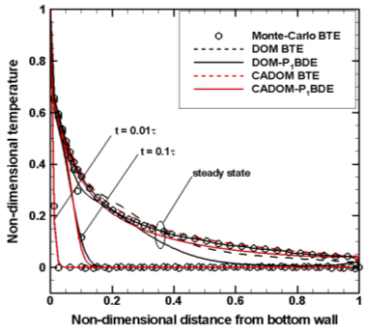

Figure 3: Centerline temperature distributions at Knudsen number of 1.

Results for Knudsen number of 100 (ballistic limit) are shown in Fig. 4. The "ray effect" is very pronounced in this case for the standard DOM, as is evident from the oscillations in the temperature profiles, and more so from the heat flux distributions at the top wall. As evident from Fig. 3(b), CADOM alleviates the ray effects tremendously. For this particular Knudsen number, distinct slips in temperature are observed at the walls, indicative of strongly non-equilibrium transport. The results of the current hybrid approach match solutions of the BTE quite accurately, as long as the CADOM method is used to solve for the ballistic component.

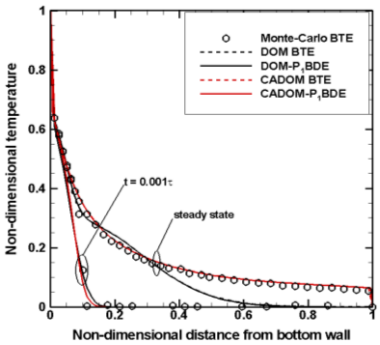

(a) Temperature along centerline

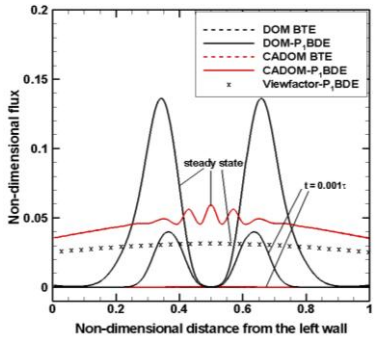

(b) Heat flux along top wall

Figure 4: Non-dimensional temperature [= $(T-T_C)/(T_H-T_C)$ ***] and heat flux [=*** $q/\sigma_p(T_H^4-T_C^4)$ ***] for Knudsen number of 100 (ballistic limit)***

The ray effect, exhibited by the standard DOM, is more clearly evident in the steady state temperature distributions shown in Fig. 5. It is clear that in this method, the energy streaks along discrete directions. The effect is alleviated tremendously by the CADOM method, which integrates the governing equation over solid angles prior to solution of the equations, thereby smoothening out the directional variation in the intensity.

Overall, based on the results obtained for this particular test case, it can be concluded that the new BDE formulation produces results that are quite accurate at all Knudsen numbers both for unsteady and steady cases. The results produced by the hybrid method (new BDE formulation), based on the CADOM method for solution of the ballistic component (CADOM-P_1), appears to be the most accurate. However, the hybrid method required about one-fifth the CPU time compared to the direct solution of the BTE using CADOM, for reasons discussed earlier. Therein lies the advantage of the hybrid method.

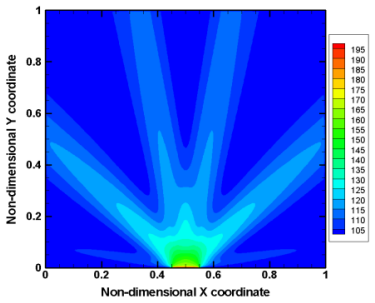

(a) Standard discrete ordinates based hybrid method (DOM- P_1***)***

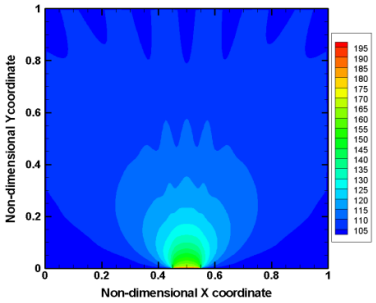

(b) Control angle discrete ordinates based hybrid method (CADOM- P_1***)***

Figure 5: Comparison of steady state temperature distributions obtained using DOM and CADOM based hybrid methods for Knudsen number of 100.

SUMMARY AND CONCLUSIONS

A new generalized form of the ballistic-diffusive equations (BDE) for approximate solution of the Boltzmann Transport Equation (BTE) for phonons is presented and demonstrated. This new formulation does not require *a priori* knowledge of the specific heat capacity of the material. The only input required in this formulation is the scattering time scale (or Knudsen number in non-dimensional form), which is the same input required for solution of the original BTE. In this work, the ballistic component of the phonon intensity is determined by the solving the governing equation using two different established methods that are appropriate for use in complex geometries, namely the discrete ordinates method (DOM), and the control angle discrete ordinates method (CADOM). To demonstrate the method, a two-dimensional transient heat conduction problem is solved. Results of each method for solving the BDE are compared against benchmark Monte Carlo results, as well as solutions of the BTE using standalone DOM and CADOM at various Knudsen numbers. It is found that standalone CADOM (for BTE) and hybrid CADOM-P_1 (for BDE) yield the best accuracy. The hybrid CADOM-P_1 is found to be the best method in terms of computational efficiency. Standard DOM is found to be unacceptable at large Knudsen numbers (ballistic limit) due to "ray effects".

ACKNOWLEDGMENTS

Financial support for this work was provided in part by the Department of Energy's Basic Energy Science Program through Grant Number DE-FG02-06ER46330.

REFERENCES

[1] Ju, Y.S., and Goodson, K. E., (1999), ''Phonon Scattering in Silicon Films with Thickness of Order 100 nm,'' *Appl. Phys. Lett*., 74, No. 20, pp. 3005-3007

[2] Tien, C.L., Majumdar, A., and Gerner, F.M., eds., 1998, *Microscale Energy Transport*, Taylor and Francis.

[3] G. A. Bird, (1994), *Molecular Gas Dynamics and the Direct Simulation of Gas Flows*, Claredon, Oxford

[4] Mazumder, S. and Kersch, A., (2000), "A Fast Monte-Carlo Scheme for Thermal Radiation in Semiconductor Processing Applications," *Numerical Heat Transfer, Part B: Fundamentals*, Vol. 37(2), pp. 185-199.

[5] Maltby, J.D. and Burns, P.J., (1991), "Performance, Accuracy, and Convergence in a Three-Dimensional Monte Carlo Radiative Heat Transfer Simulation," *Numerical Heat Transfer, Part B: Fundamentals*, Vol. 19(2), pp. 191-209.

[6] Fischetti, M.V. and Laux, S.E., (1993), "Monte Carlo Study of Electron Transport in Silicon Inversion Layers," *Physical Review B*, Vol. 48, No. 4, pp. 2244.

[7] Jacoboni, C. and Reggiani, L., (1983), "The Monte Carlo Method for the Solution of Charge Transport in Semiconductors with Applications to Covalent Materials," *Reviews of Modern Physics*, Vol. 55, No. 3, pp. 642-705.

[8] Mazumder, S., and Majumdar, A., (2001), "Monte Carlo Study of Phonon Transport in Solid Thin Films Including Dispersion and Polarization," *Journal of Heat Transfer*, Vol. 123, pp. 749-759

[9] Lacroix, D., and Joulain, K., and Lemonnier, D. (2005), "Monte Carlo transient phonon transport in Silicon and Germanium at nanoscale," *Phys. Rev. B*, Vol. 72, 064305(1-11)

[10] Mittal, A., and Mazumder, S., (2010), "Monte Carlo Study of Phonon Heat Conduction in Silicon Thin Films Including Contributions of Optical Phonons," *Journal of Heat Transfer*, Vol. 132, Article number 052402.

[11] Narumanchi, S.V.J., (2003), "Simulation of heat transport in sub-micron conduction", *PhD. Dissertation*, Department of Mechanical Engineering, Carnegie Mellon University.

[12] Narumanchi, S.V.J., Murthy, J.Y., Amon, C.H., (2004), "Sub-micron heat transport model in silicon accounting for phonon dispersion and polarization," *Journal of Heat Transfer*, Vol. 126, pp. 946-955

[13] Murthy, J.Y., Narumanchi, S.V.J., Pascual-Gutierrez, J.A., Wang, T., Ni, C. and Mathur, S.R., (2005) "Review of Multi-Scale Simulation in Sub-Micron Heat Transfer", *International Journal for Multiscale Computational Engineering*, Vol. 3, pp. 5-32

[14] Fiveland, W., (1988), "Three-dimensional Radiative Heat Transfer Solutions by the Discrete Ordinates Method*," Journal of Thermophysics and Heat Transfer*, Vol. 2(4), pp. 309-316.

[15] Raithby, G.D., and Chui, E.H., (1990), "A Finite-Volume Method for Predicting a Radiant Heat Transfer in Enclosures with Participating Media," *Journal of Heat Transfer*, Vol. 112(2), pp. 415-423.

[16] Chai, J.C., Lee, H.S. and Patankar, S.V., (1994), "Finite-Volume Method for Radiative Heat Transfer," *Journal of Thermophysics and Heat Transfer*, Vol. 8, pp. 419-425

[17] Chai, J.C., Lee, H.S., and Patankar, S.V., (1993), "Ray effect and false scattering in the discrete ordinates method," *Numerical Heat Transfer, Part B*, Vol. 24, pp. 373-389

[18] Gaskell, P.H, Lau, A.K.C., (1988), "Curvature-compensated convective transport: SMART, a new boundedness preserving transport algorithm," *International Journal for Numerical Methods in Fluids*, Vol. 8, pp. 617–641

[19] Modest, M.F., (2003), *Radiative Heat Transfer*, Second Edition, Academic Press.

[20] Ravishankar, M., Mazumder, S., and Kumar, A., (2010), "Finite-Volume Formulation and Solution of the P_3 Equations of Radiative Transfer on Unstructured Meshes," *Journal of Heat Transfer*, Vol. 132, Article number 023402.

[21] Modest, M.F., and Yang, J., (2008), "Elliptic PDE formulation and boundary conditions of the spherical harmonics method of arbitrary order for general three-dimensional geometries," *Journal of Quantitative Spectroscopy and Radiative Transfer*, Vol. 109, pp. 1641-1666.

[22] Olfe, D.B., (1967), "A modification of the differential approximation for radiative transfer," *AIAA Journal*, Vol. 5(4), pp. 638-643

[23] Modest M.F., (1989), "The modified differential approximation for radiative transfer in general three-dimensional media," *Journal of Thermophysics and Heat Transfer*, Vol. 3(3), pp. 283-288

[24] Chen, G., (2001), "Ballistic-Diffusive Heat Conduction Equations," *Phys. Rev. Lett.*, Vol. 86, pp. 2297-2230.

[25] Chen, G., (2002), "Ballistic-Diffusive Equations for Transient Heat Conduction from Nano to Macroscales," *Journal of Heat Transfer*, Vol. 124, pp. 320-328.

[26] Yang, R., Chen, G., Laroche, M., and Taur, Y., (2005), "Simulation of Nanoscale Multidimensional Transient Heat Conduction Problems Using Ballistic-Diffusive Equations and Phonon Boltzmann Equation," *Journal of Heat Transfer*, Vol. 127, pp. 298-306.

[27] Ravishankar, M., Mazumder, S., and Sankar, M., (2010), "Application of the Modified Differential Approximation for Radiative Transfer to Arbitrary Geometry," *Journal of Quantitative Spectroscopy and Radiative Transfer*, Vol. 111, pp. 2052-2069.

[28] Kittel, C., (1986), *Introduction to Solid State Physics*, John Wiley & Sons Inc., Sixth Edition

[29] Whitaker, S., (1983), *Fundamental Principles of Heat Transfer*, Krieger Publishing Company.

[30] Murthy, J.Y., and Mathur, S.R., (1998), "Finite-Volume Method for Radiative Heat Transfer Using Unstructured Meshes," *Journal of Thermophysics and Heat Transfer*, Vol. 12(3), pp. 313-321.

[31] Saad, Y., (2003), *Iterative Methods for Sparse Linear Systems*, 2nd Edition, SIAM, Philadelphia, PA.